Processing of Al-Si Waste Contaminated with Iron by Powder Metallurgy

Vojtěch Kučera, Vojtěch Dalibor
Department of Metals and Corrosion Engineering, University of chemistry and technology Prague, Technická 5, 16628 Prague 6, Czech Republic. E-mail: kucerao@vscht.cz

Hot dip aluminizing of steel products leads to the contamination of the batch by iron, which could significantly exceed its admissible levels. The re-processing of thus-polluted Al-Si waste by conventional casting technologies requires extensive technological adjustments, which raise the cost. Therefore, powder metallurgy was used to process Al-Si15-Fe7 alloy (in wt. %) to refine the microstructure and improved mechanical properties without further modification of chemical composition. Mechanical machining (MM) followed by spark plasma sintering (SPS) led to strong improvement of ductility, whereas mechanical machining coupled with high-energy ball milling (HEBM) and consolidation by SPS resulted in compressive strength reaching almost 1000 MPa, but with the absence of plastic deformation. In addition, both samples showed no significant change in mechanical properties even after long-term annealing at 400 °C.

Keywords: Al-Si waste, recycling, mechanical machining, high-energy ball milling, spark plasma sintering

1 Introduction

Hot dip aluminizing is widely used method for covering the steel sheets or other steel products with heat and oxidation resistant coatings in automotive industry. However, the batch is enriched mainly by iron, which can greatly exceed the admissible levels during the hot dipping. The increased iron content hinders the recycling of such polluted batch and significantly raises the cost of processing [1-3].

The steel sheets are aluminized in continuous process, where sheets are immersed into the batch of molten aluminium for a certain period of time. The reaction between the steel sheet and the molten aluminium leads to a forming of an intermetallic layer on the surface of steel by atomic inter-diffusion. Subsequently, the residual aluminium liquid forms a top layer of coating having the same composition as a melt, which may consist of pure aluminium or an Al-Si melt [4,5]. The kinetics of the coating process as well as the thickness of the coating are influenced by temperature of the batch, chemical composition of the substrate and the batch [6]. Whereas, the coating is formed during the reaction, iron dissolves at the same time and contaminates the melt. The contamination of the melt can rise up to 7% of iron, while the admissible level of iron is usually about 1% for pressure die casting, where the higher concentration is desirable [7]. Nevertheless, the critical iron content for most applications in Al-Si cast alloys should not exceed 0.5% [8].

The negative effect of Fe is its low solubility in aluminium solid solution, which leads to the formation of brittle intermetallic phases with platelet-like morphology. These phases cause stress concentration under the applied stress, which can result in premature failure due to the micro-crack initiation and growth [7,9-11]. In binary Al-Fe system, the detrimental phase is monoclinic Al_3Fe phase (also reported as $Al_{13}Fe_4$) and in ternary Al-Si-Fe system, it is monoclinic/orthorhombic $Fe_2Al_9Si_2$ (β-Al_5FeSi) phase. Their harmful effect on both strength and ductility may be affected by the size, distribution and morphology [7,10].

However, a reliable and economic method to suppress the negative influence of iron has not yet been available in industrial scale. Y. Osawa et al. [12] investigated the influence of cooling rate and ultrasonic vibration on morphology and size of the intermetallic compounds during the crystallization in Al-xSi-Fe7 (in wt. %) alloy. The increasing cooling rate did not change the morphology of the Al-Si-Fe phases and resulted in the phase narrowing. The application of ultrasonic vibration led to the refinement of the iron intermetallic compounds, which crystallized preferably from the melt. It is known that the ultrasonic vibration promotes nucleation and fine particle structure during solidification at nucleation temperature. Recently, several solid state recycling techniques have been developed. These techniques use consolidation by plastic deformation to process the small-size Al scrap such as chips and cutting, which suffer from substantial oxidation during the re-melting by conventional methods. A.E. Tekkay et al. [13] processed chips from milling and turning of AA 6060 by direct hot extrusion. The billets made from recycled chips evinced similar mechanical properties and microstructure as the hot extruded conventionally cast billets. The billets prepared in [14] from the chips of the same aluminium alloy by ECAP revealed also promising mechanical properties. D. Paraskevas et al. [15] used chips 6061 to „dilute“ the gas atomised powder of the same alloy, which was consolidated by spark plasma sintering (SPS). The fully compact samples had homogeneous properties, where atomised powder acted as binding material for the chips.

The aim of this study is to design a method for processing of Al-Si alloy highly contaminated with Fe without change in the chemical composition. We chose powder metallurgy as a promising way to prepare such alloy with a very fine microstructure and required mechanical properties. Compared to the aforementioned studies, we used Al-Si ingot highly contaminated by iron originating from the hot dip aluminizing to produce chips by mechanical machining. These chips were processed by two methods: i) cold pre-compaction and spark plasma sintering (SPS), ii) high-energy ball milling (HEBM), cold pre-

compaction and SPS. The compact samples were compared to the conventionally as-casted alloy with the same chemical composition. Moreover, thermal stability could be expected due to the low diffusion coefficients of iron in aluminium solid solution and relatively high volume fraction of intermetallic phases [16].

2 Materials and Methods

The commercial ingot of Al-Si-Fe alloy obtained from external supplier was processed by powder metallurgy in our experiment. The ingot was casted from the Al-Si bath used for steel hot dip aluminizing, which was highly contaminated by Fe. The chemical composition of the as-received ingot is shown in Tab 1. Two approaches were chosen for processing of the Al-Si-Fe alloy (Fig. 1). In the first approach, the ingot was mechanically machined by the file to produce chips (Fig. 2a), which were subsequently consolidated by SPS FCT Systeme HP-D 10. The batch of chips was 10 g and was placed into the graphite die with 20 mm in diameter. The chips were first preloaded by a force of 3 kN to ensure good contact between the puncher and graphite die. The heating rate was 200 °C·min^{-1} until it reached final 500 °C. After the temperature was reached, the sample was compressed by a force of 48 MPa. The total time the sample remained at the 500 °C was 10 minutes followed by a spontaneous cooling in chamber. In the second approach, the machined chips were further mechanically milled (HEBM) before the SPS consolidation. The chips were placed into a steel grinding jar together with milling balls both made from AISI 420 stainless steel, sealed and flushed with inert argon gas to prevent oxidation during milling. To reduce the cold-welding during mechanical alloying, stearic acid (0.5 wt. %) was added as the process control agent (PCA). The ball-to-powder mass ratio was 30:1. The high-energy ball milling was carried out by planetary milling device Retsch PM 100 with rotational speed of 400 rpm while the direction of rotation was reversed every 30 minutes. The overall milling time was 8 hours with 10 minutes breaks every 30 minutes. The mechanically milled powder (Fig. 2b) was then consolidated by SPS with the same aforementioned conditions.

In order to reduce porosity, the powders in the both approaches were pre-compacted by the pressure of 360 MPa for 5 minutes at the LabTest 5.250SP1-VM universal testing machine forming semi-compact samples further used for the compaction via SPS.

Chemical and phase composition was determined using X-ray fluorescence (XRF) and X-ray Diffraction (XRD) (ARL 9400 XP and PANalytical X'Pert Pro, Cu Kα1 λ=1.54059 • 10^{-10} m) analyses.

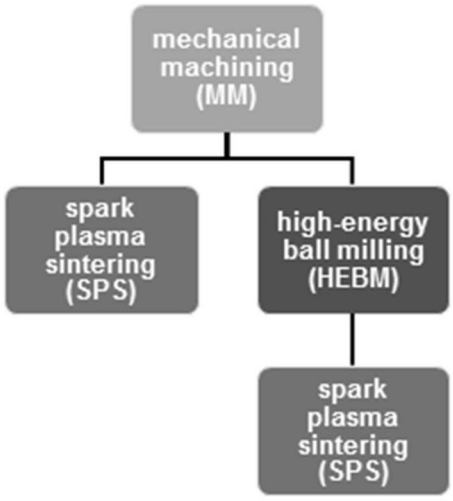

Fig. 1 *Schematic representation of individual preparation processes.*

Tab. 1 *Chemical composition (in wt. %) of Al-Si-Fe ingot given by XRF.*

Element	Al	Si	Fe	Ni	Cu
[wt. %]	Balance	14.27	7.18	0.52	0.22

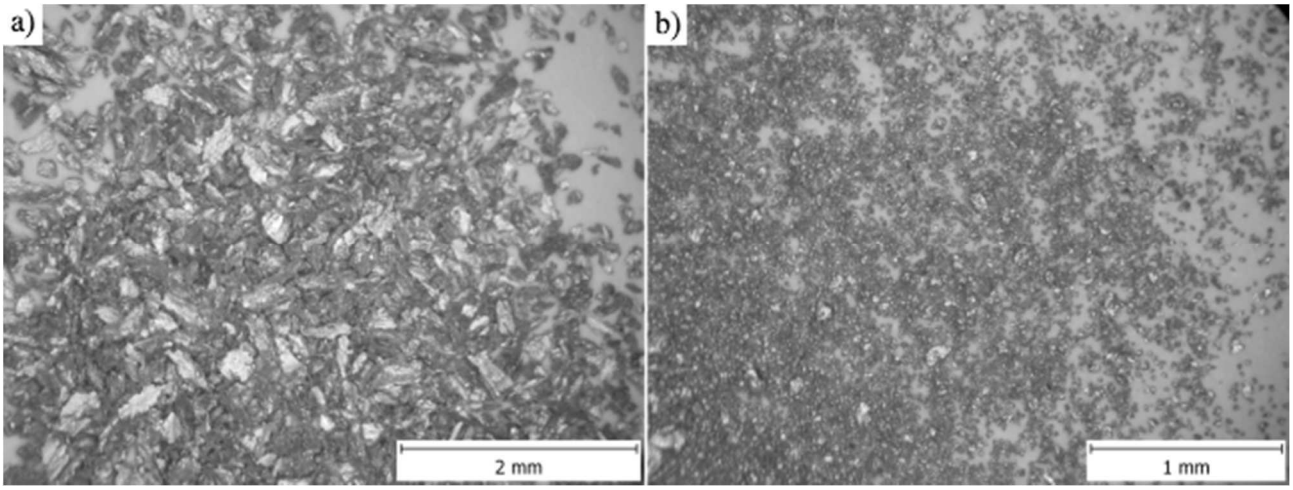

Fig. 2 *The morphologies of Al-Si-Fe chips a) and chips after 8h of high-energy ball milling b)*

Samples for microstructure observation were prepared by standard metallography procedure including grinding, polishing and etching the samples in Keller reagent (190 ml distilled water, 5 ml HNO_3, 3 ml HCl, 2 ml HF). Microstructure was observed by optical microscope (Olympus PME-3) and scanning electron microscope (Tescan Vega 3 LMU, 20 kV, SE + BSE detectors) equipped with energy dispersive spectroscopy detector

(Oxford Instruments INCA 350, 20 mm^2). Mechanical properties of prepared alloys were evaluated on the basis of compression tests performed at room temperature. To verify the thermal stability, samples were annealed for 100 hours at temperature of 400 °C. The Al-Si-Fe alloy was simultaneously prepared by conventional casting technology. The ingot was re-melted in electric resistance furnace and then casted into a brass mould to form ingot of 50 mm in diameter and 150 mm in height. Thus-prepared alloy was used without further processing as a reference material.

3 Results and Discussion

The phase composition of as-received Al-Si-Fe ingot consisted of solid solution α-Al, Si particles and ternary intermediate phase $Fe_2Al_9Si_2$ (Fig. 3). The ternary phase is commonly reported in literature [8,9,17] as β-Al_5FeSi ($Al_{4.5}FeSi$ stoichiometrically) with the monoclinic/orthorhombic structure [7]. As was expected, the phase composition of both the MM and even the MM +HEBM was identical with the as-cast alloy. Only peak broadening was observed (Tab. 2), which was more evident in the MM + HEBM powder. The peak broadening in the case of the MM + HEBM (Tab. 2) represented by the full-width half maxima (FWHM) of 111 peak was 0.307 compared to the as-cast alloy with the FWHM of 0.154. This could be attributed to the plastic deformation during mechanical machining [18] and milling, which introduced internal stresses into the lattice and moreover to the grain refinement. After SPS consolidation, no new phases were observed and peak narrowing occurred due to the relaxing of internal stresses.

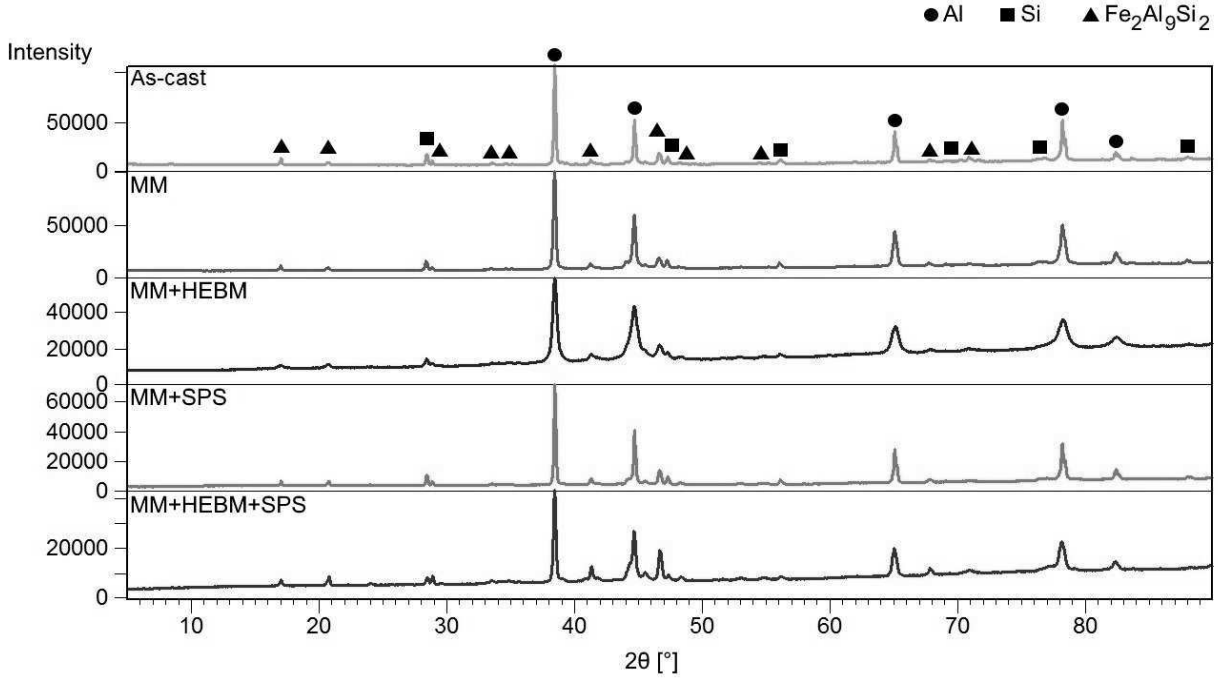

Fig. 3 *The XRD pattern of processed Al-Si-Fe alloy (as-cast; MM – mechanically machined; HEBM – mechanically milled; SPS – spark plasma sintering).*

Tab. 2 *The summary of the results of XRD analysis (2θ – diffraction angle; FWHM – full width at Half maximum).*

Route of processing	2θ [°] Al (1 1 1)	FWHM Al (1 1 1)
As-cast	38.476	0.154
MM	38.457	0.192
MM + HEBM	38.472	0.307
MM +SPS	38.459	0.135
MM + HEBM +SPS	38.429	0.179

The microstructure of the as-cast ingot (Fig. 4a) consisted of eutectic α-Al + Si and large platelets of $Fe_2Al_9Si_2$ with several hundreds of micrometres in size, which appears as needle in 2D projection. The cooling rate and chemical composition have the main impact on the size and volume fraction of the intermetallic phases during solidification. Increasing Fe content leads to the earlier formation of the ternary Al-Si-Fe intermetallic phases, which could solidify prior to dendrites of α-Al solid solution or independently at the same time. Simultaneously, it increases the volume fraction of these phases, which tend to grow up to several hundreds of micrometres. Moreover, considerable amount of voids and cracks were observed in the microstructure of as-cast alloy [10,12]. Shabestari et al [7] stated that large iron-containing phases formed prior to the eutectic mixture α-Al+Si tended to prevent the flow of the melt and may cause the increased porosity.

After the mechanical machining, the $Fe_2Al_9Si_2$ phase preserved its platelet-like morphology, but it was fragmented into much finer particles with a relatively diverse size (Fig. 4b). It could be expected that such refinement would have beneficial effect on mechanical properties, especially on ductility. Even more significant refinement was achieved by combination of mechanical machining and HEBM (Fig. 4c), which contained sub-micron and some relatively larger particles (bright).

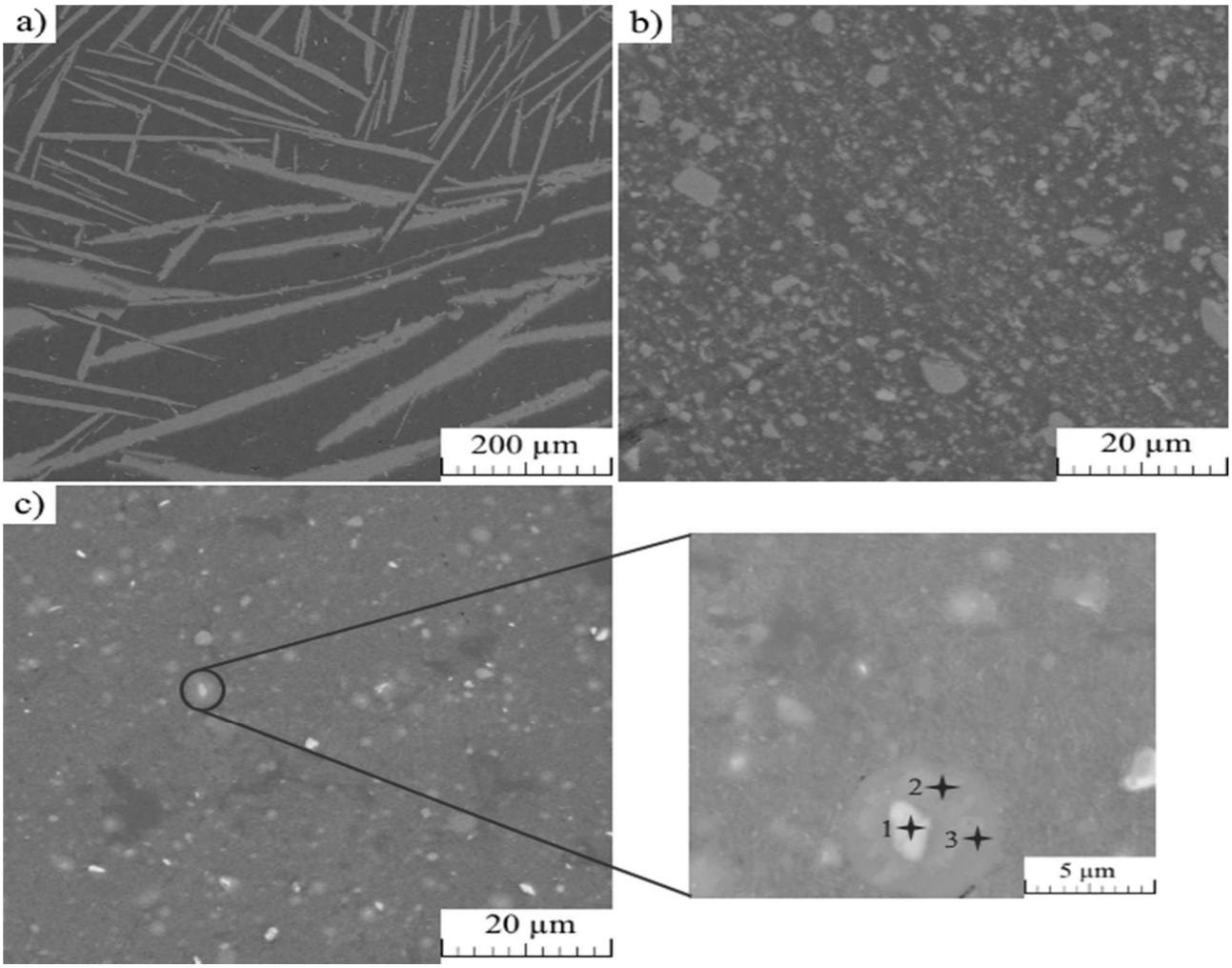

Fig. 4 *The microstructure of the samples prepared by: a) casting (as-cast); b) mechanical machining and spark plasma sintering (MM +SPS) and c) mechanical machining followed by high-energy ball milling and spark plasma sintering (MM + HEBM +SPS).*

To determine the chemical composition of larger particles (bright) in the MM + HEBM +SPS, the EDS point analysis of chemical composition was performed (Tab. 3). The analysed particles (red circle in Fig. 4c) were binary Al-Fe and ternary Al-Si-Fe phases rich in Fe, where the Fe content decreased from the centre to the edge of the particle. The centre of the particle (bright) containing the highest amount of Fe could correspond to $Fe_3(Al_{1-x}Si_x)$, while the adjacent area (light grey) had equimolar amount of Al and Fe, which might be identified as $Fe(Al_{1-x}Si_x)$. These phases were observed to form as a solid layers next to pure iron particles [19,20]. The edge of the particle (dark grey) was probably the β-Al_5FeSi. The origin of the intermediate particles can be attributed to the contamination from the stainless steel milling jar and balls considering also the small amount of Cr. However, due to the limited resolution of the EDS detector, the chemical composition of the phases could be influenced by the surrounding.

Tab. 3 *The SEM-EDS point analysis of chemical composition of the MM + HEBM +SPS sample in atomic percent.*

Point n.	Al	Si	Fe	Cr	Identified phases
1	27.7	12.2	59.8	0.3	$Fe_3(Al_{1-x}Si_x)$
2	43.6	12.8	43.1	0.3	$Fe(Al_{1-x}Si_x)$
3	72.2	11.5	15.4	-	β-Al_5FeSi

To evaluate the mechanical properties and thermal stability of the samples, the compression stress-strain test were carried out at laboratory temperature (Fig. 5a) and after 100 h of annealing at 400 °C (Fig. 5b). The results of compression stress-strain test of samples without annealing (Tab. 4) showed significant improvement of ductility after mechanical machining. This improvement, which was approximately 20%, was caused by the considerable fragmentation of $Fe_2Al_9Si_2$ phase. This phase is brittle with high hardness compared to ductile α-Al solid solution. In as-cast alloy, platelet phases work as stress concentrators due to the notch effect and have relatively low bond strength with the matrix, which could result in decohesion failure [8]. The important factor could be also

increased porosity of the as-cast sample. Breaking up of the large platelets led to decrease of its detrimental notch effect and thus to ductility increase. The highest compression strength (CS) had the MM + HEBM +SPS sample. The CS reached 997 MPa, but with the low ductility. The reason for the absence of ductility could be found in high-energy ball milling. This process leads to the high deformation of material, and therefore, to high internal stresses and concentration of crystalline defects.

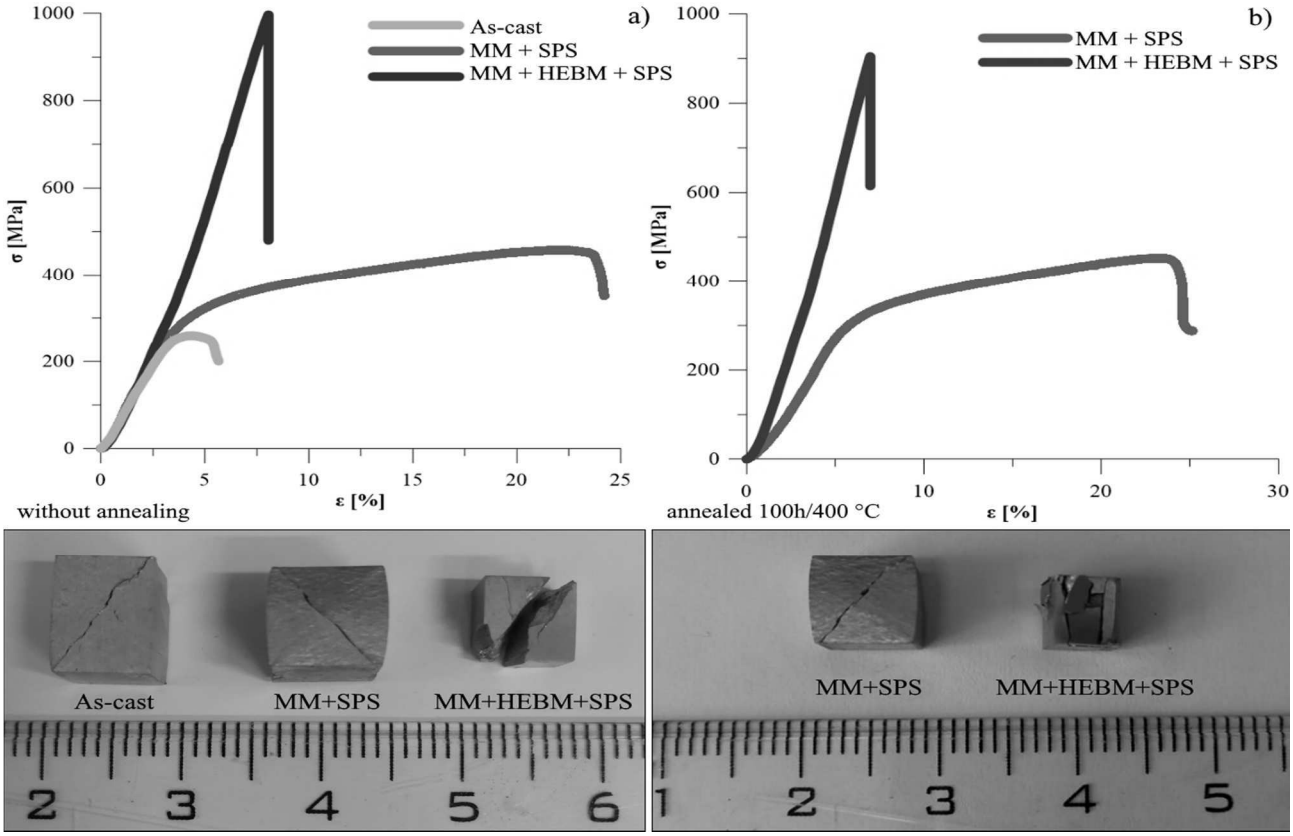

Fig. 5 *The results of compression stress-strain test of the unaffected samples a) and after 100h of annealing at 400 °C b) (CYS – compression yield stress, CS – compression strength, ε – relative deformation).*

After the annealing (400 °C, 100h), the mechanical properties remained almost unchanged (Tab. 4), which indicated thermal stability of the alloy. The MM +SPS maintained its strength and relatively high ductility. On the other hand, the MM + HEBM +SPS evinced a mild drop of the CS (about 92 MPa). The explanation can be found in relieving the internal stresses, introduced from high-energy ball milling, caused by elevated temperature during long annealing period. Although, the decrease of the CS was not significant and the sample still showed a good thermal stability. The diffusion coefficient of iron is much lower than aluminium in α-Al solid solution and even than silicon [16]. Thus, its increased content could play an important role in Al-Si-Fe thermal stability [21].

Tab. 4 *The results from compression tests at laboratory temperature and after 100 h annealing at 400 °C (CYS-compressive yield strength, CS-compressive strength, ε - relative deformation).*

Route of processing	Laboratory temperature			400 °C		
	CYS [MPa]	CS [MPa]	ε [%]	CYS [MPa]	CS [MPa]	ε [%]
As-cast	242	260	5.65	-	-	-
MM +SPS	300	458	24.21	294	453	25.15
MM + HEBM +SPS	-	997	8.05	-	905	6.96

4 Summary

The Al-Si waste with high iron contamination was successfully processed by powder metallurgy. Compared to conventional casting technologies, the mechanical machining followed by the SPS (the MM +SPS) and the mechanical machining in combination with the high-energy ball milling and the SPS consolidation (the MM + HEBM +SPS) led to the significant fragmentation and refinement of the coarse intermediate β-Al_5FeSi phase. This phase is considered as the most harmful one, especially due to its negative effect on ductility. In spite of this, the MM + SPS evinced strong improvement in ductility and higher strength than its as-casted equivalent, whereas the MM + HEBM + SPS considerably exceed the strength of the other two samples, but with the absence of plastic deformation. Moreover, the high content of iron could led to improved thermal stability.

These results indicate that even such polluted Al-Si waste from hot dip aluminizing could be processed by powder metallurgy without further modification of chemical composition and still obtain material with good mechanical properties.

Acknowledgement

The authors wish to thank the Czech Science Foundation (project no. P108/12/G043) for its financial support of this research.

References

[1] AWAN, G.H.,UL HASAN, F. (2008). The morphology of coating/substrate interface in hot-dip-aluminized steels. In: *Materials Science and Engineering: A*, Vol. 472, No. 1, pp. 157-165.

[2] LEMMENS, B., et al. (2018). Deformation induced degradation of hot-dip aluminized steel. In: *Materials Science and Engineering: A*, Vol. 710, No. Supplement C, pp. 385-391.

[3] BOLIBRUCHOVÁ, D.,BRŮNA, M. (2017). Impact of the elements affecting the negative iron-based phases morphology in aluminium alloys - Summary results. In: *Manufacturing Technology*, Vol. 17, No. 5, pp. 675-679.

[4] GUI, Z.-X., et al. (2014). Cracking and interfacial debonding of the Al–Si coating in hot stamping of pre-coated boron steel. In: *Applied Surface Science*, Vol. 316, No. Supplement C, pp. 595-603.

[5] GUI, Z.-x., et al. (2014). Thermo-mechanical behavior of the Al–Si alloy coated hot stamping boron steel. In: *Materials & Design*, Vol. 60, No. Supplement C, pp. 26-33.

[6] CHENG, W.-J.,WANG, C.-J. (2011). Effect of silicon on the formation of intermetallic phases in aluminide coating on mild steel. In: *Intermetallics*, Vol. 19, No. 10, pp. 1455-1460.

[7] SHABESTARI, S.G. (2004). The effect of iron and manganese on the formation of intermetallic compounds in aluminum–silicon alloys. In: *Materials Science and Engineering: A*, Vol. 383, No. 2, pp. 289-298.

[8] JOZEF, P. (2009). The application of Ni for improvement of Al-Si-Fe alloys. In: *Materials Engineering*, Vol. 16, No. 4, pp. 29 - 32.

[9] RAO, Y., YAN, H., HU, Z. (2013). Modification of eutectic silicon and β-Al5FeSi phases in as-cast ADC12 alloys by using samarium addition. In: *Journal of Rare Earths*, Vol. 31, No. 9, pp. 916-922.

[10] TAYLOR, J.A. (2012). Iron-Containing Intermetallic Phases in Al-Si Based Casting Alloys. In: *Procedia Materials Science*, Vol. 1, No. Supplement C, pp. 19-33.

[11] PRŮŠA, F., et al. (2017). The influence of SPS compaction pressure onto mechanical properties of Al-20Si-16Fe alloy prepared by mechanical alloying. In: *Manufacturing Technology*, Vol. 17, No. 6, pp. 936-939.

[12] OSAWA, Y., et al. (2007). Morphology of Intermetallic Compounds in Al-Si-Fe Alloy and Its Control by Ultrasonic Vibration. In: *MATERIALS TRANSACTIONS*, Vol. 48, No. 9, pp. 2467-2475.

[13] TEKKAYA, A.E., et al. (2009). Hot profile extrusion of AA-6060 aluminum chips. In: *Journal of Materials Processing Technology*, Vol. 209, No. 7, pp. 3343-3350.

[14] HAASE, M., et al. (2012). Improving mechanical properties of chip-based aluminum extrudates by integrated extrusion and equal channel angular pressing (iECAP). In: *Materials Science and Engineering: A*, Vol. 539, No. Supplement C, pp. 194-204.

[15] PARASKEVAS, D., et al. (2015). The Use of Spark Plasma Sintering to Fabricate a Two-phase Material from Blended Aluminium Alloy Scrap and Gas Atomized Powder. In: *Procedia CIRP*, Vol. 26, No. Supplement C, pp. 455-460.

[16] KHALIFA, W., SAMUEL, F.H., GRUZLESKI, J.E. (2003). Iron intermetallic phases in the Al corner of the Al-Si-Fe system. In: *Metallurgical and Materials Transactions A*, Vol. 34, No. 3, pp. 807-825.

[17] MARKER, M.C.J., et al. (2011). Phase equilibria and structural investigations in the system Al–Fe–Si. In: *Intermetallics*, Vol. 19, No. 12, pp. 1919-1929.

[18] MONKOVÁ, K., et al. (2016). Chip formation comparison-merchant's model vs.Model with rounded cutting edge. In: *Manufacturing Technology*, Vol. 16, No. 6, pp. 1320-1326.

[19] GUPTA, S.P. (2002). Intermetallic compound formation in Fe–Al–Si ternary system: Part I. In: *Materials Characterization*, Vol. 49, No. 4, pp. 269-291.

[20] MAITRA, T.,GUPTA, S.P. (2002). Intermetallic compound formation in Fe–Al–Si ternary system: Part II. In: *Materials Characterization*, Vol. 49, No. 4, pp. 293-311.

[21] PRŮŠA, F., et al. (2015). Mechanical alloying: A way how to improve properties of aluminium alloys. In: *Manufacturing Technology*, Vol. 15, No. 6, pp. 1036-1043.

DOI: 10.21062/ujep/54.2018/a/1213-2489/MT/18/1/60